SOURCE (OR PART OF THE FOLLOWING SOURCE):
Type article
Title Low-Field Optically Detected Magnetic-Resonance of a Coupled Triplet-Doublet Defect Pair in Diamond
Author(s) E. Vanoort, P. Stroomer, M. Glasbeek
Faculty UvA: Universiteitsbibliotheek
Year 1990

FULL BIBLIOGRAPHIC DETAILS:
http://hdl.handle.net/11245/1.427794

Low-field optically detected magnetic resonance of a coupled triplet-doublet defect pair in diamond

Eric van Oort, Paul Stroomer, and Max Glasbeek
Laboratory for Physical Chemistry, University of Amsterdam, Nieuwe Achtergracht 127, 1018 WS Amsterdam, The Netherlands
(Received 26 March 1990)

Microwave-induced changes in the optical emission of the N-V center in diamond have previously been attributed to magnetic resonance of the defect in its ^3A ground state [E. van Oort *et al.*, J. Phys. C **21**, 4385 (1988)]. In this paper, the focus is on the origin of the hyperfine splittings that are observed in the optically detected magnetic-resonance (ODMR) spectra at zero and low magnetic fields. Detailed analysis of the anisotropic behavior of the line splittings in a magnetic field shows that the hyperfine structure arises from triplet-doublet magnetic dipolar interactions of N-V centers and P_1 centers (with $S=\frac{1}{2}$). The ODMR spectrum of the N-V center appears to display the nitrogen hyperfine interaction characteristic of the P_1 center.

Magnetic dipole-dipole interactions have been the subject of extensive studies on pairs, triads, and higher-order groupings of ions or on aggregated defects.[1] Most studies apply electron paramagnetic resonance (EPR) spectroscopy and are almost exclusively restricted to stable $S=\frac{1}{2}$ radicals. To our knowledge, intercenter magnetic dipolar couplings involving higher spin multiplicities have not yet been observed. In this paper, the origin of additional hyperfine structure in the optically detected magnetic resonance (ODMR) of the nitrogen-vacancy defect (the N-V center) in diamond is investigated. Evidence is presented that the hyperfine structure is characteristic of dipolar coupled triplet-doublet dimers of the N-V center and a single nitrogen impurity center (the P_1 center).

In type-Ib diamond, the N-V center consists of a substitutional nitrogen atom neighboring a carbon vacancy having trapped one electron.[2] Recently, a ^3A ground state for the N-V defect has been established.[3,4] In absorption and emission, the defect gives rise to a zero-phonon transition peaking at 638 nm.[5] Optical excitation of the N-V center induces a spin alignment within its triplet ground state and microwave-induced changes in this alignment in turn induces a change in the population of the optically excited emissive E state. In this way, electron spin resonance of the ^3A ground state is optically detected.[4,6]

To create the N-V defect centers, type-Ib diamond samples were irradiated in a Van der Graaff accelerator and annealed afterwards.[5] Details of the ODMR experimental setup have been given elsewhere.[7] Figure 1(a) displays the zero-field ODMR spectrum of the N-V center at 1.4 K. The ODMR spectrum consists of a central line peaked at 2880 MHz and a few, relatively weak, side bands shifted by 70 and 140 MHz to the low- and high-frequency sides of the main transition. From Zeeman effects it has been shown[6,8] that the 2880 MHz zero-field transition corresponds to the N-V center triplet spin resonance. We now focus on the weak side bands in the ODMR spectrum of Fig. 1(a). Experiments on different samples showed that the intensity of the side bands with respect to that of the central line is not constant. From this it is concluded that the weak bands are not intrinsic to the N-V center.

Figure 1(b) shows the ODMR spectrum when the sample is placed in a magnetic field of 100 G along the crystallographic [001] axis. At higher magnetic field values, the intensity of the (hyper)fine structure lines decreased until for field strengths above about 250 G the line pattern was too weak to be observed. The measured ODMR frequencies for magnetic-field strengths up to 200 G for $\mathbf{H}\parallel$ [001] are plotted in Fig. 2. In this figure only the res-

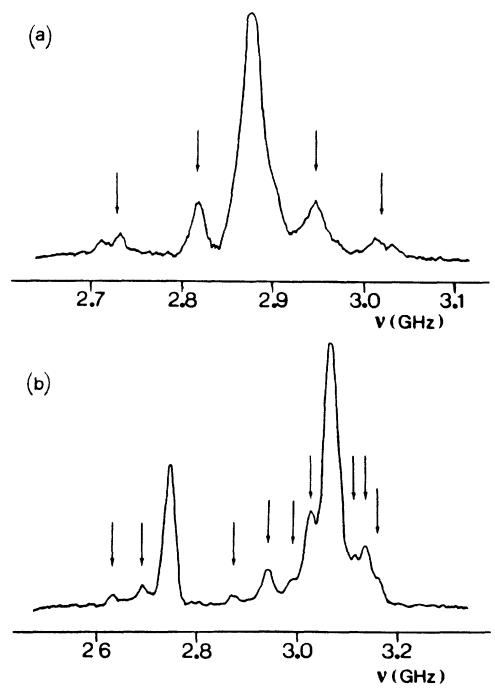

FIG. 1. Optically detected magnetic resonance (ODMR) spectrum of the N-V center at $T=1.4$ K, (a) in zero field; (b) for $\mathbf{H}\parallel[001]$, $H=100$ G. Arrows indicate side-band structures. Excitation is at 514 nm, detection wavelength is at 638 nm.

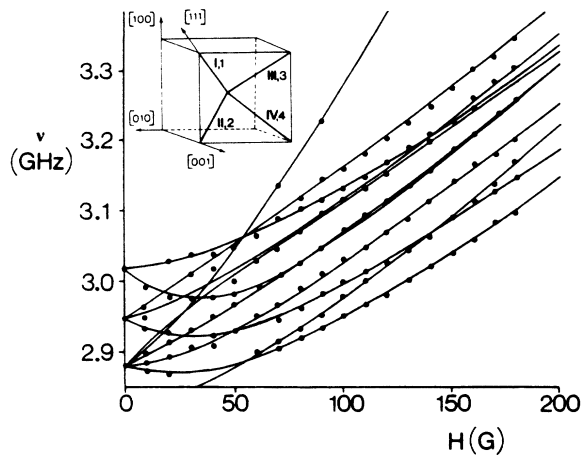

FIG. 2. Magnetic-field dependence of the microwave resonance frequency for the N-V defect in its ^3A ground state. The magnetic field is oriented parallel to a crystallographic [001] axis. All other experimental conditions as in Fig. 1. Solid lines show fits calculated from Eq. (1) and the spin-Hamiltonian parameters given in Table I. Inset shows orientation of main axes of N-V and P_1 centers, labeled I–IV and 1–4, respectively.

onance frequencies corresponding to the hyperfine lines around one of the unperturbed N-V triplet spin resonances are shown (namely the high-frequency component), because only for these hf lines the signal-to-noise ratio was such that they could easily be followed as the magnetic field was increased.

The angular variation of the ODMR peak positions, as observed in the microwave frequency range from 2800 to 3300 MHz, when a magnetic field ($H=100$ G) is rotated in the (001) plane, is represented by Fig. 3. The figure has been subdivided to facilitate the discussion in terms of defect pairs consisting of an axially symmetric N-V center (with $S=1$) and a P_1 center [with $S=\frac{1}{2}$ (Refs. 9 and 10)].

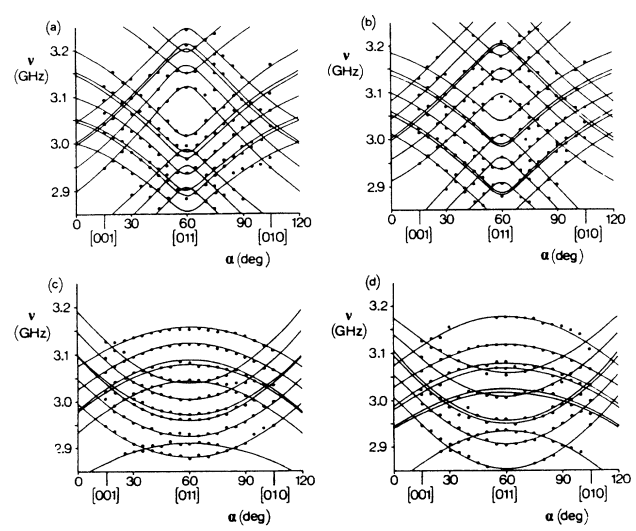

FIG. 3. Angular dependence of the ODMR transitions when the magnetic field is rotated in the (001) plane. $H=100$ G, experimental conditions as in Fig. 1. Anisotropy of pairs (a) (I,1), (I,2), (II,1), (II,2); (b) (I,3), (I,4), (II,3), (II,4); (c) (III,1), (III,2), (IV,1), (IV,2); (d) (III,3), (III,4), (IV,3), (IV,4), labeling as in Fig. 2. Solid lines in (a) to (d) show fits calculated from Eq. (1) and the spin-Hamiltonian parameters given in Table I.

We start with the spin Hamiltonian given by Kollmar and Sixl[11] for a loosely occupied triplet-doublet spin system,

$$H=D[(S_z^T)^2-\tfrac{2}{3}]+g_e^T\mu_B\mathbf{H}\cdot\mathbf{S}^T+g_e^D\mu_B\mathbf{H}\cdot\mathbf{S}^D +\mathbf{S}^D\cdot\mathsf{A}\cdot\mathbf{I}^D+\mathbf{S}^T\cdot\mathsf{T}\cdot\mathbf{S}^D\ . \tag{1}$$

In Eq. (1), D represents the zero-field splitting within the N-V center triplet state, g_e^T and g_e^D are the isotropic g values for the triplet and doublet states respectively, $\mathbf{S}^T$ and $\mathbf{S}^D$ represent the triplet and doublet electronic spin operators, $\mathbf{I}^D$ represents the spin operator of the nitrogen nucleus of the P_1 center, A is a second-rank tensor representing the intrinsic electron-nuclear hyperfine interaction of the P_1 center, and T is the tensor characteristic of the triplet-doublet magnetic dipole-dipole interactions. The nuclear quadrupole interaction of the nitrogen nucleus of the P_1 center,[10] and the electron-nuclear hyperfine couplings of the N-V center,[2] are on the order of a few MHz only and henceforth need not be considered.

The triplet-doublet interactions will be considered in first order only, i.e.,

$$\mathbf{S}^T\cdot\mathsf{T}\cdot\mathbf{S}^D\cong S_z^T T_{zz} S_z^D+S_z^T T_{zx} S_x^D\ , \tag{2}$$

where T_{zz}, T_{zx} are the triplet-doublet interaction constants defined as

$$T_{zz}=\frac{g_e^T g_e^D(\mu_B)^2}{r_{TD}^3}(3\cos^2\vartheta-1)\ , \tag{3a}$$

$$T_{zx}=\frac{g_e^T g_e^D(\mu_B)^2}{r_{TD}^3}3\sin\vartheta\cos\vartheta\ , \tag{3b}$$

where ϑ is the angle between the triplet state molecular main axis and the line joining the triplet and doublet magnetic dipoles. Computer fits of the experimental data were obtained using the spin-Hamiltonian parameter values given in Table I. The calculated results are displayed by the drawn lines in Fig. 3. For the N-V center as well as the P_1 center the defect main axis is oriented along one of the four [111] crystallographic directions of the diamond lattice. Thus, in all, 16 magnetically different triplet-doublet pair defects are possible for an arbitrary direction of the applied magnetic field.

TABLE I. Values of spin Hamiltonian parameters of the N-V center and P_1 center as used in simulations of ODMR anisotropy.

Parameter	Numerical value	Reference
$\lvert D\rvert$	2880 MHz	2,6,8
g_e^T	2.0028±0.0003	2
g_e^D	2.0024±0.0005	9
$A_\parallel$	113.984 MHz	9,10
$A_\perp$	81.344 MHz	9,10
T_{zz}, T_{zx}	1–10 MHz	this work

When the magnetic field is in the (001) plane, however, only four magnetically inequivalent pairs of N-V and P_1 centers can be distinguished. The angular dependences of the low-field ODMR lines of the four pairs are presented distinctly in Figs. 3(a)–(d). From a comparison with the experimental data in the same figure, it is concluded that the triplet-doublet pair center model is in satisfactory agreement with the experimental results. For completeness we remark that the quality of the simulations was not influenced when the values of the parameters T_{zz} and T_{zx} were changed in the range from 1 to 10 MHz.

A major finding of this work is that side-band splittings in the zero- and low-field ODMR spectra of the N-V center are to a large extent determined by the intrinsic hyperfine interactions of the P_1 center dipolar coupled to the probed N-V center. We now examine in a little more detail how the P_1-hyperfine splittings are transferred to the spin resonances of the N-V center. We make use of the simplified spin level scheme depicted in Fig. 4, in which the $m_S=0$ and $m_S=\pm 1$ spin levels of the N-V center in zero field are considered. In the absence of triplet-doublet interactions, the P_1-center spin energies are added as three hyperfine split doublets. In zero field this P_1-hyperfine splitting is

$$\Delta E=\tfrac{1}{2}[(A_{\parallel}^2+A_{\perp}^2)]^{1/2} .$$

The doublet spin functions are specified in Table II in terms of $|m_S,m_I\rangle$ basis functions (with $m_S=\pm\frac{1}{2}$, and $m_I=-1,0,1$). Consider now the influence of the triplet-doublet interactions, which are taken to be small compared to the hyperfine interactions of the P_1 center. It is first noted that the triplet-doublet terms of Eq. (3) do not affect the levels belonging to the $m_S=0$ manifold. In the $m_S=\pm 1$ manifolds, however, the operator $S_z^T T_{zz} S_z^D$ mixes the spin function $|\psi_1\rangle$ with $|\psi_3\rangle$ and $|\psi_5\rangle$, and $|\psi_2\rangle$ with $|\psi_4\rangle$ and $|\psi_6\rangle$, and a small splitting as indicated on the right-hand side of the energy scheme of Fig. 4 ensues. As a result of the dipolar-induced mixing, spin resonances peaking near

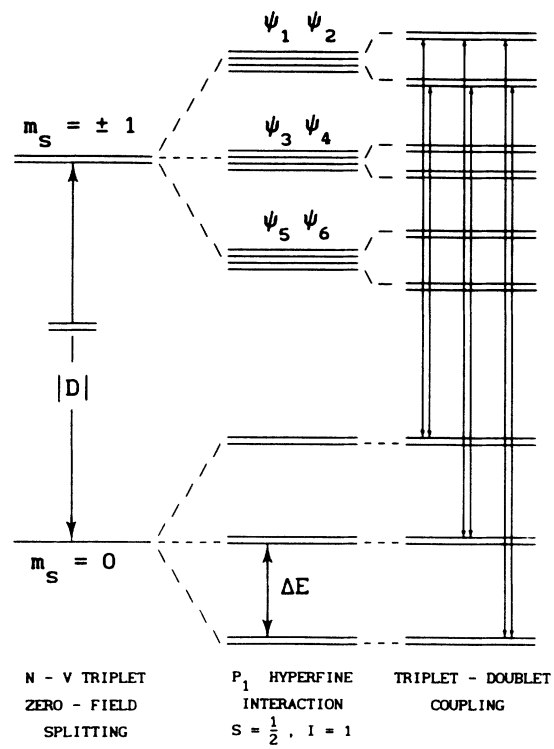

FIG. 4. Schematic energy level diagram for the N-V center in the ^3A ground state in zero field, showing the splitting of the $m_S=0$ and $m_S=+1$ triplet spin manifolds due to the interaction with a P_1 doublet spin. Spin transitions at frequencies of $|D|$, $|D|+\frac{1}{2}[(A_{\parallel}^2+A_{\perp}^2)]^{1/2}$ and $|D|+[(A_{\parallel}^2+A_{\perp}^2)]^{1/2}$ are indicated.

$$|D|+\tfrac{1}{2}[(A_{\parallel}^2+A_{\perp}^2)]^{1/2}$$

and

$$|D|+[(A_{\parallel}^2+A_{\perp}^2)]^{1/2} ,$$

additional to the main resonance at $|D|$, become partially

TABLE II. Eigenfunctions ψ_l of the P_1 center as expressed in terms of $|m_S,M_I\rangle$ ($m_S=\pm\frac{1}{2}, M_I=-1,0,+1$) basis functions and with $\eta\equiv\arctan(A_{\perp}/A_{\parallel})$.

$$\psi_l=[\tfrac{1}{2}(\cos\eta+1)]|\tfrac{1}{2},1\rangle-[\tfrac{1}{2}(\cos\eta-1)]|\tfrac{1}{2},-1\rangle+\left[\frac{1}{\sqrt{2}}\sin\eta\right]|-\tfrac{1}{2},0\rangle$$

$$\psi_2=\left[\frac{1}{\sqrt{2}}\sin\eta\right]|\tfrac{1}{2},0\rangle-[\tfrac{1}{2}(\cos\eta-1)]|-\tfrac{1}{2},1\rangle+[\tfrac{1}{2}(\cos\eta+1)]|-\tfrac{1}{2},-1\rangle$$

$$\psi_3=\left[-\frac{1}{\sqrt{2}}\sin\eta\right]|\tfrac{1}{2},1\rangle+\left[\frac{1}{\sqrt{2}}\sin\eta\right]|\tfrac{1}{2},-1\rangle+(\cos\eta)|-\tfrac{1}{2},0\rangle$$

$$\psi_4=(\cos\eta)|\tfrac{1}{2},0\rangle+\left[\frac{1}{\sqrt{2}}\sin\eta\right]|-\tfrac{1}{2},1\rangle-\left[\frac{1}{\sqrt{2}}\sin\eta\right]|-\tfrac{1}{2},-1\rangle$$

$$\psi_5=[\tfrac{1}{2}(\cos\eta-1)]|\tfrac{1}{2},1\rangle-[\tfrac{1}{2}(\cos\eta+1)]|\tfrac{1}{2},-1\rangle+\left[\frac{1}{\sqrt{2}}\sin\eta\right]|-\tfrac{1}{2},0\rangle$$

$$\psi_6=\left[\frac{1}{\sqrt{2}}\sin\eta\right]|\tfrac{1}{2},0\rangle-[\tfrac{1}{2}(\cos\eta+1)]|-\tfrac{1}{2},1\rangle+[\tfrac{1}{2}(\cos\eta-1)]|-\tfrac{1}{2},-1\rangle$$

allowed (cf. Fig. 4). When considering the influence of the $S_z^T T_{zx} S_x^D$ term of Eq. (2), essentially no new additional features are anticipated.

Since the N-V and P_1 defects are dispersed randomly in the diamond lattice and many differently coupled pairs with a large variation in intercenter distances r_{TD} and angles ϑ exist, there is an almost continuous distribution of the small triplet-doublet splittings. Thus the splittings associated with the triplet-doublet dipolar coupling are not resolved in the ODMR spectrum, but instead they contribute to inhomogeneous broadening of the ODMR lines only. This explains also for the observation that in samples with a larger concentration of the nitrogen impurity, a larger ODMR line width is found. In high magnetic fields, the triplet and doublet spin systems become decoupled. As a result, no hyperfine splitting characteristic of the triplet-doublet interactions are observed in the high-field EPR spectra of the N-V center.[12] Likewise, the contribution of the triplet-doublet magnetic dipolar couplings to the inhomogeneous line broadening has vanished and, for example, in X band the width of the N-V center EPR lines becomes small enough (FWHM is $\sim$0.5 G) to resolve a nitrogen nuclear spin hyperfine coupling of 0.83 G.

We thank Drukker International (Amsterdam) for the donation of type-Ib diamond samples. This work has been supported in part by the Netherlands Foundation for Chemical Research (SON) with financial aid from the Netherlands Organization for Scientific Research (NWO).

[1]See, e.g., W. Hayes and A. M. Stoneham, *Defects and defect processes in nonmetallic solids* (Wiley, New York, 1985); B. Henderson and G. F. Imbusch, *Optical Spectroscopy of Inorganic Solids* (Clarendon, Oxford, 1989).

[2]J. H. N. Loubser and J. H. van Wyk, Diamond Res. **11**, 4 (1977).

[3]N. R. S. Reddy, N. B. Manson, and E. R. Krausz, J. Lumin. **38**, 46 (1987).

[4]E. Van Oort, N. B. Manson, and M. Glasbeek, J. Phys. C **21**, 4385 (1988).

[5]G. Davies and M. F. Hamer, Proc. R. Soc. A **348**, 285 (1976).

[6]E. van Oort and M. Glasbeek, Phys. Rev. B **40**, 6509 (1989); Chem. Phys. **143**, 131 (1990).

[7]M. Glasbeek and R. Hond, Phys. Rev. B **23**, 4220 (1981).

[8]P. D. Bloch, W. S. Brocklesby, R. T. Harley, and M. J. Henderson, J. Phys. (Paris) Colloq. **46**, C7-527 (1985).

[9]W. V. Smith, P. P. Sorokin, T. L. Gelles, and G. J. Lasher, Phys. Rev. **115**, 1546 (1959).

[10]R. J. Cook and D. H. Whiffen, Proc. R. Soc. A **295**, 99 (1966).

[11]C. Kollmar and H. Sixl, Mol. Phys. **45**, 1199 (1982).

[12]E. van Oort, R. Sitters, and M. Glasbeek (unpublished).